



INTERNATIONAL ATOMIC ENERGY AGENCY
UNITED NATIONS EDUCATIONAL, SCIENTIFIC AND CULTURAL ORGANIZATION



INTERNATIONAL CENTRE FOR THEORETICAL PHYSICS
34100 TRIESTE (ITALY) • P.O.B. 586 • MIRAMARE • STRADA COSTIERA 11 • TELEPHONE: 2260-1
CABLE: CENTRATOM • TELEX 600892-1

SMR.378/14

WORKSHOP ON THEORETICAL FLUID MECHANICS AND APPLICATIONS
(9 - 27 January 1989)

FLOW IN POROUS MEDIA

by

D. S. Riley (University of Bristol, U.K.)

FLOW IN POROUS MEDIA

D.S. RILEY
Northwestern University
Evanston, IL 60208
U.S.A.

These are preliminary lecture notes, intended only for distribution to participants

PREAMBLE

The subject of this part of the workshop concerns the transport of fluid through a porous medium i.e. through a solid matrix (more simply, a solid structure with holes in it). By their nature, porous media are extremely complex and, in consequence, so are the flows through them. Thus it is not surprising that many simplifying assumptions are made in our mathematical models, and that there are important areas of the subject which are controversial and not yet modelled satisfactorily. We can not hope in this brief introduction to cover all the important areas, nor can we address all the multifarious issues.

A moments reflection on the following will give some indication, perhaps, why our goals can not be too ambitious:

The solid matrix may be rigid or deformable - the deformation may be elastic, or follow some other more exotic constitutive relation, and the holes may be occupied by multiphase, miscible or immiscible fluids. Each phase may be made up of several components, which may or may not be interacting between themselves and the solid matrix. The processes may be isothermal, or non-isothermal with very small or very large temperature variations; there may be phase changes. Capillary forces may be important - moving contact lines may feature (e.g. in secondary oil-recovery problems). The media may be homogeneous, heterogeneous, multilayered, ... The list is seemingly endless, and it makes one wonder why there is such interest in this area. A few examples will illustrate where transport in porous media is encountered:

- Civil Engineering
 - flow and pollution of ground water; movement of moisture and heat through building materials

- Soil Mechanics
 - soil compaction and subsidence
- Oil Reservoir Engineering
 - non-isothermal multiphase flow of gas and oil; enhanced oil recovery techniques
- Geothermal Reservoir Engineering
 - electricity production; district heating schemes
- Chemical Engineering
 - packed-bed catalysis; filtration
- Agriculture
 - irrigation of crops; spread of nutrients
- Waste Management
 - filtration; waste disposal.

In all of these, decisions relating to the design, construction and operation of systems are required. Rate and location of water injection in an oil reservoir, rate of pumping/rate of recharge of aquifers, and the siting of radioactive waste depositories are just a few examples. These problems are mathematically very challenging. Mathematical models are relatively easy to formulate, but much harder to justify. Then we have the problem of determining the parameters to insert into our models. Unfortunately results of laboratory tests on small samples (about one metre in length, say) rarely scale up to field conditions (where the scale may be several kilometres).

Having emphasized the challenging nature of the subject, let me also stress that it is possible to make good progress, provided one accepts and acknowledges the limitations of our mathematical models.

The aim of this short introduction is to familiarize you with the basic concepts, to outline the equations governing convection in saturated porous media, and then to consider an application drawn (loosely) from radioactive waste disposal modelling.

INTRODUCTION

As already alluded to in the preamble, a porous medium is a solid which is full of holes. Usually the number of holes, or rather pores, is sufficiently large and randomly distributed in size, etc. that a volume average is needed to make sensible progress. In describing flow phenomena we are mainly interested in interconnected pores, since these are the ones which permit flow. Dead-end pores, i.e. ones with only one opening, are important in certain phenomena, for example absorption of pollutants into the solid. Totally enclosed pores can affect certain other problems, for example when the compressibility of the medium is important, or when there is a high concentration of them and heat transport properties are affected. POROSITY is a quantitative property that describes the fraction of the medium that is taken up by the various types of hole.

Consider some location \underline{r}_0 in the porous medium, and consider a sphere (say) centred on \underline{r}_0 . We can take the ratio of the void volume (V_{void}) to the total volume (V) of the sphere, and plot it against V , for varying V as shown

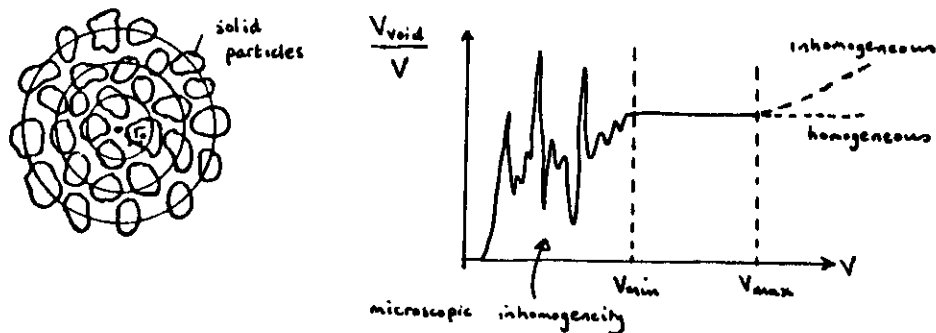


Figure 1

If the sample volume V is too low, the ratio is sensitive to V ; when V lies between V_{min} and V_{max} , the ratio has been statistically smoothed and the ratio is fairly constant. When $V > V_{\text{max}}$ the ratio senses the large scale variations that occur in inhomogeneous material. We take the ratio V_{void}/V with $V_{\text{min}} < V < V_{\text{max}}$ as our definition of the porosity, and denote it by ϵ .

This discussion has introduced us to the idea that "macroscopic" quantities can be derived by averaging "microscopic" (this does not mean molecular) quantities over a suitable volume. This volume is usually called a REPRESENTATIVE ELEMENTARY VOLUME (or REV in short). This idea should be familiar from discussion (for example in G. Batchelor's book: An Introduction to Fluid Dynamics) on the continuum hypothesis in fluid dynamics; in the present case we are averaging over larger scales. To be useful, the REV must satisfy the following criteria:

- (i) Where ever the REV is placed within the porous medium domain, it should contain both solid phase and void space;
- (ii) The void space should contain some multiply-connected subdomain;
- (iii) The averaged parameter should be statistically meaningful.

The analysis of flow and heat transfer is usually based on the transport equations resulting from differential balance laws, i.e. conservation laws, applied to small volumes. The prediction of global effects such as flow resistance or heat flux from a given system normally requires detailed information on both velocity and temperature fields. For a continuous medium, this information is extracted from the solution of the "microscopic" transport equation (Navier-Stokes and energy equations),

subject to appropriate initial and boundary conditions. When the flow is through a complex structure such as a porous medium, these equations are generally still valid within the pores, but the geometric complexity of the flow domains makes it quite impossible to solve for the detailed velocity and temperature fields. To get around this difficulty, physical phenomena in porous media are generally described by "macroscopic equations" valid over some REV. The resultant averaged equations govern suitably averaged variables such as velocity, pressure and temperature.

Darcy Velocity (or filtration velocity or seepage velocity)

In porous media, the interstitial or pointwise fluid velocity \underline{v} is not a useful entity, since it is volume fluxes that easily measured and relevant. The natural velocity to use is the so-called Darcy velocity, which is defined by

$$q = \frac{1}{S} \int_S \underline{v} \cdot d\mathbf{S}$$

where S is the total boundary area (including solid portions) of the REV:

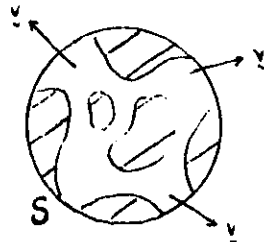


Figure 2

It is usually assumed that the average interstitial velocity and the Darcy velocity are related by:

$$q = \epsilon \underline{v}$$

where ϵ is the porosity.

Darcy's law

The basic equation governing fluid flow in porous media expresses conservation of momentum. Darcy's law (1856) relates the volumetric flow rate Q flowing through a porous medium directly to the energy loss, inversely to the height of the medium, and proportional to a factor termed the HYDRAULIC CONDUCTIVITY (K). The figure illustrates schematically the kind of experiment Darcy performed.

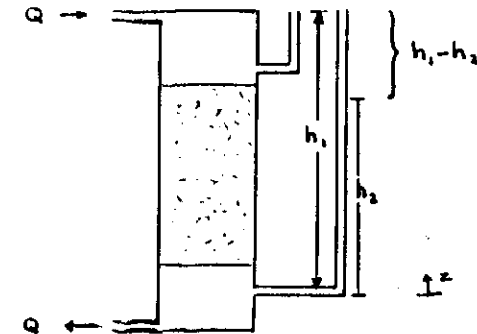


Figure 3

Here fluid enters a packed sandbed, of length Δl and cross-sectional area A , at the top and flows through the system at a volumetric flowrate Q . The difference in the hydraulic heads at the top and the bottom of the bed is

measured by water manometers. This difference is given ^{by} $h_1 - h_2$. Darcy's law is

$$Q = \frac{KA(h_1 - h_2)}{\Delta l} = \frac{KA(h_{\text{top}} - h_{\text{bottom}})}{\Delta l}$$

where $h = z + p/\rho g$ is the hydraulic head. This result is empirical - it is derived by experimental observation. Note that:

- (i) if there were no sandbed (i.e. no porous medium) the relation would involve Q^2 (and not Q), assuming the flow to be inviscid;
- (ii) the relation is analogous to the Poiseuille law when gravity is absent.

The hydraulic conductivity K is dependent on the properties of the fluid, as well as the pore structure of the medium. It is usual to replace the hydraulic conductivity by an intrinsic permeability k defined by

$$K = \frac{k\rho g}{\mu}$$

where k is the permeability of the porous medium and in principle is only a function of the pore structure; μ is the coefficient of viscosity of the fluid. The hydraulic conductivity is temperature dependent, since the properties of the fluid (density and viscosity) are temperature dependent; the intrinsic permeability is not temperature dependent.

Darcy's law is often written in differential form so that in one-dimension:

$$\frac{Q}{A} = q = - \frac{k}{\mu} \left(\frac{dp}{dz} + \rho g \right) \quad \text{in the } z\text{-direction}$$

where q is the Darcy speed. It is usually assumed that Darcy's law is valid in three dimensions, that k is a second-order tensor, dependent upon the directional properties of the pore structure, and q is a vector given by

$$q = - \frac{k}{\mu} \nabla p, \text{ ignoring gravity.}$$

Often, in practice, the porous medium is assumed to be homogeneous and isotropic, so that

$$q = - \frac{k}{\mu} \nabla p$$

i.e. the tensor can be replaced by a scalar.

Validity of Darcy's Law

Darcy's law is usually considered valid for creeping flow where the Reynolds number for a porous medium is smaller than unity. In order to define this Reynolds number, we introduce the concept of hydraulic radius, which is defined (if the medium is particulate in nature) as the void volume of a porous medium divided by the surface area of the medium. Suppose the medium is made up of regular spherical particles, each one having volume V_p and surface area S_p , and hence diameter D_p such that

$$D_p = \frac{6V_p}{S_p}$$

Now if ϵ is the porosity of the medium

$$\epsilon = \frac{\text{void volume}}{\text{total volume}} = \frac{\text{void volume}}{(\text{void volume} + \text{volume of particles})}$$

hence void volume = $\frac{\epsilon}{1-\epsilon}$ (volume of particles). Thus the hydraulic radius R_H

is given by

$$R_H = \left(\frac{\epsilon}{1-\epsilon} \right) \frac{NV_p}{NS_p} = \frac{\epsilon D_p}{6(1-\epsilon)}$$

where N = number of particles. For nonspherical particles, the effective particle diameter can be defined by $6V/S$, where V is the volume of the particle and S its surface area.

The Reynolds number is now defined as:

$$\begin{aligned} Re &= \frac{vK}{\nu} \\ &= \frac{q}{\epsilon} \frac{\epsilon D_p}{6(1-\epsilon)\nu} \\ &= \frac{qD_p}{6(1-\epsilon)\nu} \end{aligned}$$

where v = interstitial velocity ($= q/\epsilon$), and $\nu = \mu/\rho$ is the kinematic viscosity of the saturating fluid. Usually, in fact, the numerical constant is omitted and we take

$$Re^* = \frac{qD_p}{(1-\epsilon)\nu}$$

Darcy's law is considered valid for $Re^* < 1$.

N. B. If the porous material is fibrous, then the hydraulic diameter is defined as $4A/P$, where A = cross-sectional area and P = length of perimeter.

Theoretical Derivations of Darcy's Law

There have been many attempts to place Darcy's law on a firm theoretical foundation. Two noteworthy approaches are those of J. B. Keller [1], who uses a multiple-scales approach, and of J. Bear and Y. Bachmat [2], who use averaging techniques. Both approaches start from the Navier-Stokes equations.

Deviations from Darcy's Law

a) When the Reynolds number exceeds unity, inertia effects become important. Typically for $1 < Re^* < 10$, Darcy-type experiments (without gravity) give results as shown in Figure 4.

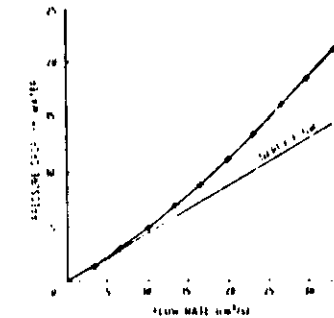


Figure 4

Instead of the linear Darcy law, there is a nonlinear (quadratic) relationship. Based on a variety of theoretical and experimental investigations, attempts have been made to develop general expressions describing the nonlinear pressure-flow relationship in porous media (see Scheidegger [3] and Bear [4]). One of the earlier expressions was developed by Forchheimer [5], based on semi-theoretical observations of nonlinear flow in tubes. Forchheimer proposed a quadratic equation of the form

$$\frac{dP}{dz} = \frac{\mu}{k} q + \frac{Fg}{k} q^2$$

which generalizes to:

$$-\nabla p = \frac{\mu}{k} \mathbf{q} + \frac{k\rho}{k} \mathbf{q}\mathbf{q}$$

where \mathbf{q} is the Darcy velocity.

This form is by no means generally applied - many workers simply take over the form of the convective derivative occurring in the Navier Stokes equations, i.e.

$$\rho \left\{ \frac{1}{\epsilon} \frac{\partial \mathbf{q}}{\partial t} + \frac{1}{2} (\mathbf{q} \cdot \nabla) \mathbf{q} \right\} = -\nabla p - \frac{\mu}{k} \mathbf{q} + \rho \mathbf{g}.$$

This form has been the subject of criticism in the literature - the criticism arises from the fact that modelling the inertia this way increases the order of the governing equations and can lead to ill-posed problems.

(b) Another controversial area of modelling in porous media concerns the effect of surrounding impermeable boundaries, if present. The Darcy equation leads effectively to an inviscid (or potential) theory - e.g. if $\mathbf{q} = -\frac{k}{\mu} \nabla p$ and the fluid is incompressible so that $\nabla \cdot \mathbf{q} = 0$ (see later), then $\nabla^2 p = 0$. Thus no-slip conditions which are usually imposed on fluids at solid boundaries cannot be applied. To get round this difficulty, many use a model attributed to Brinkman [6] - essentially we just add back in the usual viscous term of the Navier-Stokes equation, eg.

$$\rho \left\{ \frac{1}{\epsilon} \frac{\partial \mathbf{q}}{\partial t} + \frac{1}{2} (\mathbf{q} \cdot \nabla) \mathbf{q} \right\} = -\nabla p - \frac{\mu}{k} \mathbf{q} + \rho \mathbf{g} + \mu \nabla^2 \mathbf{q}.$$

This has been justified for highly porous media, but Nield [7] has demonstrated its limitations for less porous media.

Equation of Continuity (conservation of mass)

The equation of continuity follows by volume averaging the usual single-fluid equation:

$$\frac{\partial \rho}{\partial t} + \text{div}(\rho \mathbf{v}) = 0.$$

Without going into the details, we may simply replace the actual fluid velocity \mathbf{v} by the Darcy equivalent $\frac{1}{\epsilon} \mathbf{q}$, giving

$$\epsilon \frac{\partial \rho}{\partial t} + \text{div}(\rho \mathbf{q}) = 0.$$

Dispersion

Before discussing the equation governing heat transfer within a porous medium, we need to review a process which is peculiar to porous media, namely that of dispersion. Transfer processes in porous media are complicated by the complex pore network. In addition to being advected along by the mean Darcy velocity, and diffused by molecular action, heat (and mass) are spread or dispersed by local variation in the flow profile across individual pores (hydrodynamic dispersion), and by the different twisted, tortuous paths inevitably followed by fluid elements which are near neighbours and travelling with similar velocities at some stage (mechanical dispersion). Hydrodynamic dispersion is equivalent to the well-known Taylor dispersion [8] in tubes:

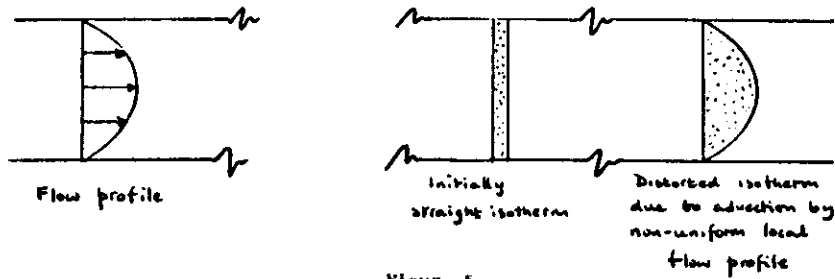


Figure 5a

Mechanical dispersion:

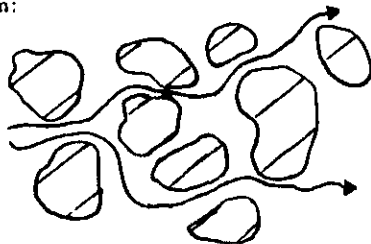


Figure 5b

The analyses of these processes are difficult. The net mathematical effect is that "diffusion coefficients" become velocity-dependent tensor quantities. Even in an isotropic medium, it is found that longitudinal (streamwise) dispersion is usually greater than transverse dispersion. To illustrate the nature of dispersion, consider a 'blob' of heat injected into a medium. In a static pure fluid, the blob would simply spread out (diffuse) spherically. In a uniform stream of pure fluid, it would be convected along as a (growing) spherical blob. In a 'uniform' flow in a porous medium, however, the blob would be distorted into an ellipsoid:

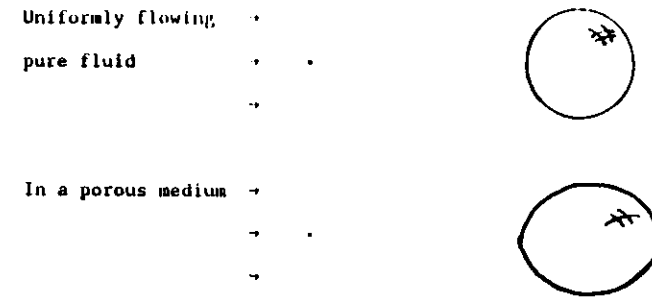


Figure 6

In practice, the coefficients in the dispersion tensor are difficult to determine, and so most people work with some constant effective scalar dispersion (or diffusion) coefficient. We shall also do this.

Energy Equation

As far as the thermal behaviour of a porous medium is concerned, for any geometrical point and its associated REV, we can define two average temperatures: T_s for the solid phase and T_f for the fluid. In mathematical modelling, two alternate methods are used depending on the difference between T_s and T_f . In the first method, the difference is assumed to be negligible, and the thermal behaviour is described by one equation for the average temperature $T = T_s = T_f$. This approach (which is the common one) is considered valid when the flow velocity is not too high and solid and fluid phases are well mixed. The second method, which applies when the difference is significant, uses two equations linked by interphase heat transfer terms.

Underlying the model equations are the following simplifying assumptions:

- the solid matrix is homogeneous, non-deformable and chemically inert with respect to the fluid;
- the fluid is single phase and Newtonian; its density varies only with temperature and not with pressure;
- no heat sources or sinks are present; thermal radiation and viscous dissipation are negligible.

When $T_s = T_f$, we have

$$(\rho c)_m \frac{\partial T}{\partial t} + (\rho c)_f (\mathbf{q} \cdot \mathbf{V})T - \lambda \nabla^2 T$$

where

$$(\rho c)_m = \epsilon (\rho c)_f + (1-\epsilon)(\rho c)_s.$$

Here $(\rho c)_f$ and $(\rho c)_s$ are the heat capacities of the fluid and solid phases (at constant pressure); λ is the effective diffusion coefficient for the saturated medium (replaces the dispersion tensor). When $T_s \neq T_f$, we take:

$$(1-\epsilon)(\rho c)_s \frac{\partial T_s}{\partial t} = \lambda_s \nabla^2 T_s + h(T_f - T_s),$$

$$\epsilon(\rho c)_f \frac{\partial T_f}{\partial t} + (\rho c)_f (\mathbf{q} \cdot \mathbf{V})T_f = \lambda_f \nabla^2 T_f + h(T_s - T_f)$$

where h is the heat transfer coefficient between the two phases. Note that $\lambda = \lambda_s + \lambda_f$, and that the determination of λ_s , λ_f and h is very difficult, both from theoretical and experimental viewpoints.

In free convection problems, the Oberbeck-Boussinesq approximations are generally invoked, i.e.

- the thermophysical properties of the saturating fluid ρ , μ , and coefficient of cubical expansion α are assumed to be constant, except in the buoyancy term (in the momentum equation) where variations in fluid density drive the motion.

The following linearized equation of state is generally assumed:

$$\rho = \rho_0 [1 - \alpha(T - T_0)]$$

where the subscript denotes some reference state.

Thus, to summarize, a typical model set of equations governing free convection is

$$\nabla \cdot \mathbf{q} = 0$$

$$\epsilon \frac{\partial \mathbf{q}}{\partial t} + \rho_0 \frac{(\mathbf{q} \cdot \mathbf{V})\mathbf{q}}{2} = - \nabla p + \rho_0 \frac{\mu}{k} \nabla^2 \mathbf{q}$$

$$(\rho c)_m \frac{\partial T}{\partial t} + (\rho c)_f (\mathbf{q} \cdot \mathbf{V})T - \lambda \nabla^2 T$$

$$\rho = \rho_0 [1 - \alpha(T - T_0)]$$

These equations may be made dimensionless by using:

length scale	-	H
time scale	-	$\frac{(\rho c)_m H^2}{\lambda}$
velocity scale	-	$\frac{\lambda}{(\rho c)_f H}$
pressure scale	-	$\frac{\lambda \mu}{k(\rho c)_f H}$
temperature scale	-	ΔT

yielding

$$\nabla \cdot \mathbf{q} = 0$$

$$\frac{M}{Pr} \left\{ \frac{1}{\epsilon} \frac{\partial}{\partial t} + \frac{1}{2} (\mathbf{u} \cdot \nabla) \right\} \mathbf{u} = - \nabla p - \mathbf{u} + Ra T \hat{\mathbf{k}}$$

$$\frac{\partial T}{\partial t} + (\mathbf{u} \cdot \nabla) T = \nabla^2 T$$

with $\hat{\mathbf{k}} = \mathbf{g}^{-1} \mathbf{g}$, and $p = P + \rho_0 g z$. The dimensionless groups appearing in

these equations are:

$$Ra = \frac{\alpha k g (\rho c)_f}{\nu \lambda} H \Delta T \quad - \quad \text{the filtration, or Darcy -, Rayleigh number}$$

$$Pr = \frac{\nu (\rho c)_f H^2}{\lambda k} \quad - \quad \text{the filtration, or Darcy -, Prandtl number}$$

$$M = \frac{(\rho c)_f}{(\rho c)_m} \quad - \quad \text{heat capacity ratio}$$

In most applications $Pr \gg 1$ and so the inertia terms are neglected. In consequence, free convection in porous media depends on the Darcy-Rayleigh number, on initial and boundary conditions, and on geometrical parameters such as aspect ratios.

Boundary Conditions

- Hydrodynamic conditions: (i) on an impermeable surface the normal velocity component is zero: $\mathbf{q} \cdot \mathbf{n} = 0$
 (\mathbf{n} normal to surface)
- (ii) at a free surface, the pressure is constant.

- Thermal conditions: (i) isothermal boundary, $T = \text{constant}$
 (ii) Adiabatic or perfectly insulating:

$$\frac{\partial T}{\partial n} - \mathbf{n} \cdot \nabla T = 0.$$

In layered media, there should be continuity in temperature and also in the normal fluxes of mass and temperature at the interfaces.

Application

1. Introduction

As an example of the application of the model equations, we examine the two-dimensional porous-medium analogue of the classical Rayleigh-Benard problem, known as the Lapwood problem [9]. Specifically, we consider a two-dimensional rectangular container of height H and width W , and filled with saturated porous material. The lateral boundaries of the container are adiabatic (i.e. perfectly insulating), while the upper and lower boundaries are held at isothermal (constant) temperatures $T_0 - \Delta T/2$, $T_0 + \Delta T/2$, respectively, where $\Delta T > 0$ so that the container is heated from below.

All boundaries are assumed impermeable

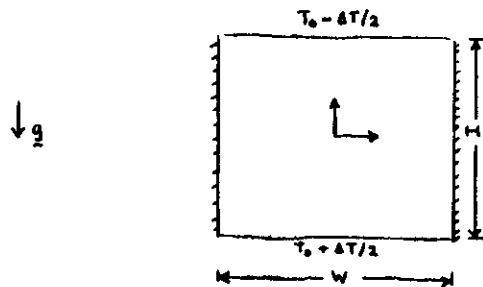


Figure 7

The problem may be thought of as a very crude model of either the flow induced by an underground radioactive waste depository, or a simple geothermal flow.

On invoking the Boussinesq approximation, and assuming that the Darcy-Prandtl is large, convective flow is governed by the equations:

$$\nabla \cdot \mathbf{q} = 0 \quad (1.1)$$

$$0 = -\nabla p - \frac{\mu}{k} \mathbf{q} + (\rho - \rho_0) \mathbf{g} \quad (1.2)$$

$$(\rho c)_m \frac{\partial T}{\partial t} + (\rho c)_f (\mathbf{q} \cdot \nabla) T = \lambda \nabla^2 T \quad (1.3)$$

$$\rho - \rho_0 = -\alpha \rho_0 (T - T_0) \quad (1.4)$$

with

$$\left. \begin{aligned} T &= T_0 + \Delta T/2 \\ w &= 0 \end{aligned} \right\} \quad \text{on } z = \pm H/2 \quad (1.5)$$

$$\left. \begin{aligned} \frac{\partial T}{\partial x} &= 0 \\ u &= 0 \end{aligned} \right\} \quad \text{on } x = \pm W/2 \quad (1.6)$$

The equations are put in a more convenient form by substituting (1.4) into (1.2), and by taking the curl of the resultant equation:

$$0 = \frac{\mu}{k} \text{curl } \mathbf{q} + \rho_0 \alpha (\nabla T \times \mathbf{g}) \quad (1.7)$$

This equation shows straight away that a necessary condition for no flow ($\mathbf{q} = 0$) is that $\nabla T \times \mathbf{g} = 0$ i.e. the isotherms must be perpendicular to the gravity vector. It should be emphasized that this result is quite general for Darcy-Boussinesq fluids. Now in the present two-dimensional problem we can eliminate equation (1.1) by introducing a streamfunction:

$$u = \frac{\partial \psi}{\partial z} \quad w = -\frac{\partial \psi}{\partial x} \quad (1.8)$$

$\text{curl } \mathbf{q} = \left(-\frac{\partial w}{\partial x} + \frac{\partial u}{\partial z} \right) \hat{\mathbf{i}} = \nabla^2 \psi \hat{\mathbf{i}}$, hence (1.7) and (1.3) become:

$$0 = \nabla^2 \psi + \rho_0 \frac{\alpha k}{\mu} \mathbf{g} \cdot \nabla T \quad (1.9)$$

$$(\rho c)_{0m} \frac{\partial T}{\partial t} + (\rho c)_{0f} \left(\frac{\partial \psi}{\partial z} \frac{\partial T}{\partial x} - \frac{\partial \psi}{\partial x} \frac{\partial T}{\partial z} \right) = \lambda \nabla^2 T \quad (1.10)$$

with

$$\left. \begin{aligned} T &= T_0 + \Delta T/2 \\ \psi &= 0 \end{aligned} \right\} \quad \text{on } z = \pm H/2 \quad (1.11)$$

$$\left. \begin{aligned} \partial T / \partial x &= 0 \\ \psi &= 0 \end{aligned} \right\} \quad \text{on } x = \pm W/2. \quad (1.12)$$

We now non-dimensionalize by writing

$$\left. \begin{aligned} x' &= \frac{x}{W} & z' &= \frac{z}{H} & T' &= \frac{T - T_0}{\Delta T} \\ t' &= \frac{\lambda T}{H^2 (\rho c)_{0m}} & \psi' &= \frac{(\rho c)_{0f}}{\lambda} \psi \end{aligned} \right\} \quad (1.13)$$

The governing system becomes, on dropping the primes for convenience,

$$\nabla^2 \psi = - \frac{Ra}{h} \frac{\partial T}{\partial x} \quad (1.14)$$

$$\frac{\partial T}{\partial t} + \frac{1}{h} \left(\frac{\partial \psi}{\partial z} \frac{\partial T}{\partial x} - \frac{\partial \psi}{\partial x} \frac{\partial T}{\partial z} \right) = \nabla^2 T \quad (1.15)$$

with

$$\left. \begin{aligned} T &= \frac{1}{2} \\ \psi &= 0 \end{aligned} \right\} \quad \text{on } z = \pm 1/2 \quad (1.16)$$

$$\left. \begin{aligned} \partial T / \partial x &= 0 \\ \psi &= 0 \end{aligned} \right\} \quad \text{on } x = \pm 1/2 \quad (1.17)$$

Here $h = \frac{W}{H}$ is the aspect ratio of the container, and $Ra = \frac{\alpha g k \Delta T (\rho c)_{0f}}{\nu \lambda} H$

($\nu = \mu/\rho_0$) is the Rayleigh number; $\nabla^2 = \frac{1}{h^2} \frac{\partial^2}{\partial x'^2} + \frac{\partial^2}{\partial z'^2}$.

In this problem the imposed temperatures have isotherms that we are perpendicular to the gravity vector and so there is a possibility of a no-flow solution. Setting $\psi = 0$ and $T = T(z)$ in the equations we see that there is a solution $T = -z$, which is usually called the conduction solution. This no-flow situation, however, is unstable because light, buoyant fluid underlies heavy fluid. As the applied temperature difference ΔT increases (so that the Rayleigh number increases), the fluid becomes more and more buoyant and motion is likely to set in. To test whether motion does occur, we test to see if small perturbations to the conduction solution are damped by the system or not.

2. Linear Stability Analysis.

We substitute

$$\psi = \epsilon \bar{\psi}, \quad T = -z + \epsilon \bar{T}, \quad \epsilon \ll 1 \quad (2.1)$$

into (1.14-17) and retain only terms that are linear in ϵ :

$$\nabla^2 \bar{\psi} = - \frac{Ra}{h} \frac{\partial \bar{T}}{\partial x} \quad (2.2)$$

$$\frac{\partial \bar{T}}{\partial t} + \frac{1}{h} \frac{\partial \bar{\psi}}{\partial x} = \nabla^2 \bar{T} \quad (2.3)$$

$$\left. \begin{aligned} \bar{T} &= 0 \\ \bar{\psi} &= 0 \end{aligned} \right\} \quad \text{on } z = \pm 1/2 \quad (2.4)$$

$$\left. \begin{aligned} \frac{\partial \bar{T}}{\partial x} &= 0 \\ \bar{\psi} &= 0 \end{aligned} \right\} \quad \text{on } x = \pm 1/2 \quad (2.5)$$

These linear, constant-coefficient, partial differential equations may be solved by the method of normal modes:

$$\left. \begin{aligned} \bar{\psi} &= A e^{i(lx + pz) + \sigma t} \\ \bar{T} &= B e^{i(lx + pz) + \sigma t} \end{aligned} \right\} \quad (2.6)$$

In fact to fit the boundary conditions, we need

$$\left. \begin{aligned} \bar{\psi} &= A \sin(m\pi\tilde{x}) \sin(n\pi\tilde{z}) e^{\sigma t} \\ \bar{T} &= B \cos(m\pi\tilde{x}) \sin(n\pi\tilde{z}) e^{\sigma t} \end{aligned} \right\} \quad (2.7)$$

and $m, n \in \mathbb{N}$

with $\tilde{x} = x + 1/2$, $\tilde{z} = z + 1/2$ substituting into the p.d.e's (2.2,3) gives:

$$\left. \begin{aligned} A \left[\frac{m^2 \pi^2}{h^2} + n^2 \pi^2 \right] &= - \frac{Ra}{h} m\pi B \\ \sigma B + \frac{m\pi A}{h} &= - \left[\frac{m^2 \pi^2}{h^2} + n^2 \pi^2 \right] B \end{aligned} \right\} \quad (2.8)$$

For a non-trivial solution to these equations:

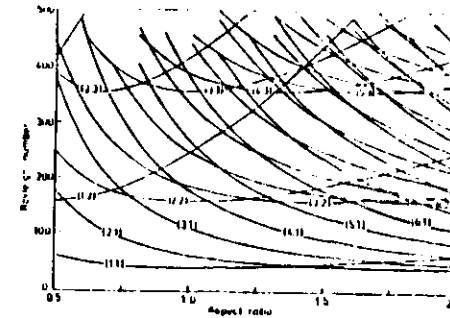
$$\begin{vmatrix} \frac{\pi^2}{h^2} (m^2 + n^2 h^2) & \frac{Ra}{h} m\pi \\ \frac{m\pi}{h} & \sigma + \frac{\pi^2}{h^2} (m^2 + n^2 h^2) \end{vmatrix} = 0 \quad (2.9)$$

or

$$Ra = \frac{\pi^2}{2h^2} (m^2 + n^2 h^2)^2 + \frac{\sigma}{m^2} (m^2 + n^2 h^2) \quad (2.10)$$

The boundary between growing disturbances ($\sigma > 0$) and decaying disturbances ($\sigma < 0$) is, of course, $\sigma = 0$, and the corresponding curve is called the neutral stability curve:

$$Ra_{m,n} = \frac{\pi^2}{2h^2} (m^2 + n^2 h^2)^2 \quad (2.11)$$



The variation of the eigenvalues $Ra_{m,n}$ with aspect ratio

Figure 8

The plot the variation of the Rayleigh number Ra with aspect ratio h for various (m,n) modes is shown in figure 8. The (m,n) mode corresponds physically to a flow with m horizontal cells and n vertical cells. Whatever the size of the container (i.e. whatever the value of h) the mode which appears first as the Rayleigh number increases from zero (i.e. heating is applied with increasing intensity) has only one cell in the vertical direction. Furthermore the smallest value of the Rayleigh number at which the (m,n) mode appears is equal to $4\pi n^2$ and this occurs when the aspect ratio is $h = m/n$. Note that the mode of lowest Rayleigh number (for a given

container) changes from $(m,1)$ to $(m+1,1)$ at an aspect ratio and Rayleigh number given by

$$h = \sqrt{m(m+1)} = H, \quad Ra = \pi^2 (2m+1)^2 / m(m+1) = Ra_H \quad (2.12)$$

Finally returning to the eigenvalue problem, we note from (2.8) that

$$B = -\frac{1}{\sqrt{Ra_{m,n}}} A, \text{ when } \sigma = 0.$$

3. Nonlinear Analysis

According to (2.6) and (2.10), the amplitude of the (m,n) mode increases exponentially when $Ra > Ra_{m,n}$. This is physically unreasonable and results from the severe approximation that we made when linearizing. When the perturbations become large, the neglected nonlinear terms are important. Palm et al [10] analyzed this post-critical situation. The idea is simple; we just continue the expansion that we started in the linear stability analysis, for Rayleigh numbers that are $O(\epsilon^2)$ away from $Ra_{m,n}$ and for fixed h . From (2.10), if

$$Ra - Ra_{m,n} = O(\epsilon^2),$$

then $\sigma = O(\epsilon^2)$. This suggests we write

$$Ra = Ra_{m,n} [1 + \epsilon^2 R_1], \quad (3.1)$$

$$\psi = 0 + \epsilon \psi^{(1)} + \epsilon^2 \psi^{(2)} + \epsilon^3 \psi^{(3)} + \dots, \quad (3.2)$$

$$T = -z + \epsilon T^{(1)} + \epsilon^2 T^{(2)} + \epsilon^3 T^{(3)} + \dots, \quad (3.3)$$

where $0 < \epsilon \ll 1$, and define $\tau = \epsilon^2 t$ as a slow-time scale. The governing equations are (2.14-17) with the $\partial T / \partial t$ term replaced by $\epsilon^2 \partial T / \partial \tau$.

We substitute (3.1-3) into the governing equations and equate powers of ϵ . At $O(\epsilon)$ the governing system is (2.2-5) with the $\partial \bar{T} / \partial t$ term missing, and the $(\bar{\psi}, \bar{T})$ replaced by $(\psi^{(1)}, T^{(1)})$. Thus,

$$\psi^{(1)} = A(\tau) \psi_{m,n}, \quad (3.4)$$

$$T^{(1)} = A(\tau) \theta_{m,n}, \quad (3.5)$$

where,

$$\begin{aligned} \psi_{m,n} &= \sin(m\pi x) \sin(n\pi z), \\ \theta_{m,n} &= \frac{-1}{\sqrt{Ra_{m,n}}} \cos(m\pi x) \sin(n\pi z). \end{aligned} \quad (3.6)$$

At $O(\epsilon^2)$ we have

$$\nabla^2 \psi^{(2)} + \frac{Ra_{m,n}}{h} \frac{\partial T^{(2)}}{\partial x} = 0, \quad (3.7)$$

$$\nabla^2 \psi^{(2)} - \frac{1}{h} \frac{\partial \psi^{(2)}}{\partial x} = \frac{1}{h} \left[\frac{\partial \psi^{(1)}}{\partial z} \frac{\partial T^{(1)}}{\partial x} - \frac{\partial \psi^{(1)}}{\partial x} \frac{\partial T^{(1)}}{\partial z} \right], \quad (3.8)$$

plus homogeneous boundary conditions; this has solution

$$\psi^{(2)} = B(\tau) \psi_{m,n}, \quad (3.9)$$

$$T^{(2)} = \frac{-m\pi^2 A^2(\tau) \sin(2n\pi z)}{8n\pi \sqrt{Ra_{m,n}}} + B(\tau) \theta_{m,n}, \quad (3.10)$$

where $B(\tau)$ is unknown.

$$\text{At } O(\epsilon^3): \quad \frac{1}{Ra_{m,n}} \nabla^2 \psi^{(3)} + \frac{1}{h} \frac{\partial T^{(3)}}{\partial x} = \frac{R_1}{h} \frac{\partial T^{(1)}}{\partial x} \quad (3.11)$$

$$\begin{aligned} \nabla^2 T^{(3)} - \frac{1}{h} \frac{\partial \psi^{(3)}}{\partial x} = \frac{1}{h} \left\{ \frac{\partial \psi^{(2)}}{\partial z} \frac{\partial T^{(1)}}{\partial x} - \frac{\partial \psi^{(2)}}{\partial x} \frac{\partial T^{(1)}}{\partial z} \right. \\ \left. + \frac{\partial \psi^{(1)}}{\partial z} \frac{\partial T^{(2)}}{\partial x} - \frac{\partial \psi^{(1)}}{\partial x} \frac{\partial T^{(2)}}{\partial z} \right\} + \frac{\partial T^{(1)}}{\partial r}. \end{aligned} \quad (3.12)$$

After a little algebra, we get

$$\frac{1}{Ra_{m,n}} \nabla^2 \psi^{(3)} + \frac{1}{h} \frac{\partial T^{(3)}}{\partial x} = \frac{m\pi R_1 A}{h/Ra_{m,n}} \sin(m\pi \tilde{x}) \sin(n\pi \tilde{z}) \quad (3.13)$$

$$\begin{aligned} \nabla^2 T^{(3)} - \frac{1}{h} \frac{\partial \psi^{(3)}}{\partial x} = \frac{m\pi^2}{h/Ra_{m,n}} \left\{ 2AB \sin(2n\pi \tilde{z}) \right. \\ \left. + \frac{mA^3}{8nh} \left[\sin(3n\pi \tilde{z}) + \sin(n\pi \tilde{z}) \right] \cos(m\pi \tilde{x}) \right\} \\ - \frac{1}{\sqrt{Ra_{m,n}}} \frac{dA}{dr} \cos(m\pi \tilde{x}) \sin(n\pi \tilde{z}). \end{aligned} \quad (3.14)$$

Multiplying (3.13) by $\psi^{(1)}$, (3.14) by $T^{(1)}$, adding the resulting equations and then integrating over the domain of the container gives a "solvability condition":

$$\frac{dA}{dr} = \frac{\pi^2 m A}{8(m+1)} \left\{ d_1 - A^2 \right\}, \quad (3.15)$$

where $d_1 = 8R_1(2m+1)/n$. When $R_1 < 0$ ($Ra < Ra_{m,n}$), there is just one steady solution to (3.14), viz. $A = 0$. When $R_1 > 0$ ($Ra > Ra_{m,n}$) there are three steady solutions: $A = 0$, $A = \pm d_1^{1/2}$. A linear stability analysis then gives the bifurcation picture shown in figure 9.

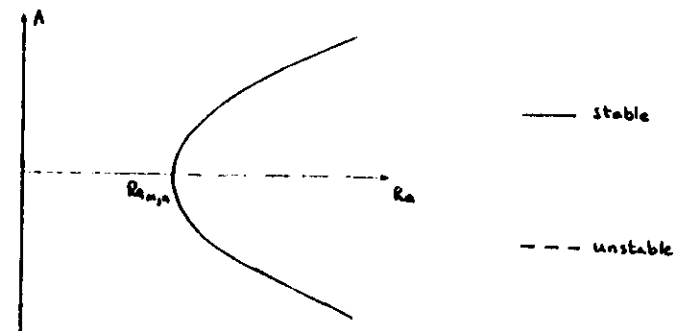


Figure 9

3. Secondary Bifurcations: Analysis Near a Double Eigenvalue

As the aspect ratio increases through one of the double eigenvalues given by (2.12), there is an exchange between primary modes with the mode of the lowest critical Rayleigh number changing from $(m,1)$ to $(m+1,1)$; in general we refer to bifurcations from the trivial branch as primary bifurcations. This type of exchange, which has been discussed in a qualitative way by Schaeffer [11], is inevitably associated with secondary bifurcations (i.e. bifurcations from a primary branch). Bauer, Keller and Reiss [12] showed how weakly nonlinear theory may be applied to analyse the local structure as the exchange takes place, and the theory was subsequently employed by Kidachi [13] in the Rayleigh-Benard problem. Here we use the theory to analyse the exchange between the leading primary modes $(m,1)$ and $(m+1,1)$ near the double eigenvalue $Ra = Ra_H$ which occurs when

$h = H$. We seek solutions to (1.14-17) in the form:

$$(\psi, \theta) = \epsilon(\psi_0, \theta_0) + \epsilon^2(\psi_1, \theta_1) + \dots, \quad (3.5)$$

$$Ra = Ra_H(1 + \epsilon^2 R_1 + \dots), \quad (3.6)$$

$$h = H(1 + \frac{1}{2}\epsilon^2 \Delta), \quad (3.7)$$

with $\Delta = \text{sgn}(h-H)$ and where ψ_1, θ_1 are functions of x, y and the slow-time scale $\tau = \epsilon^2 t$.

Proceeding as we did earlier and omitting all detail we find that:

$$(\psi_0, \theta_0) = A(\tau)(\psi_{m,1}, \theta_{m,1}) + B(\tau)(\psi_{m+1,1}, \theta_{m+1,1}), \quad (3.8)$$

where $A(\tau), B(\tau)$ are the amplitudes of the $(m,1)$ and $(m+1,1)$ modes

respectively. Applying solvability conditions to the $O(\epsilon^3)$ equations yields the evolution equations for the amplitudes:

$$\frac{dA}{d\tau} = \frac{\pi^2 m A}{8(m+1)} \{d_1 - A^2 - c_1 B^2\}, \quad (3.9)$$

$$\frac{dB}{d\tau} = \frac{\pi^2 (m+1) B}{8m} \{d_2 - c_2 A^2 - B^2\}, \quad (3.10)$$

with

$$c_1 = (4m+1)(m+1)/2m^2, \quad c_2 = m(4m+3)/(2m+1)^2, \\ d_1 = \frac{8}{m} \left\{ (2m+1)R_1 + \Delta \right\}, \quad d_2 = \frac{8}{(m+1)} \left\{ (2m+1)R_1 + \Delta \right\}. \quad (3.11)$$

The equations possess three solutions which do not depend upon the interaction of the $(m,1)$ and $(m+1,1)$ modes, viz

$$(i) \quad A = B = 0, \quad \text{trivial mode} \quad (3.12a)$$

$$(ii) \quad B = 0, \quad A^2 = d_1, \quad d_1 > 0 \quad \text{pure } (m,1) \text{ mode} \quad (3.12b)$$

$$(iii) \quad A = 0, \quad B^2 = d_2, \quad d_2 > 0 \quad \text{pure } (m+1,1) \text{ mode} \quad (3.12c)$$

The amplitude of the disturbance is zero for $Ra < \min\{Ra_1^*, Ra_2^*\}$, where

$$Ra_1^* = Ra_H \left\{ 1 + \frac{2(h-H)}{(2m+1)H} \right\}, \quad Ra_2^* = Ra_H \left\{ 1 - \frac{2(h-H)}{(2m+1)H} \right\},$$

but bifurcates at Ra_1^* and Ra_2^* . These bifurcated solutions undergo secondary bifurcation because of the presence of mixed-mode solutions in which neither A nor B are zero. These solutions are given by

$$A^2 = \frac{c_1 d_2 - d_1}{c_1 c_2 - 1}, \quad c_1 d_2 - d_1 > 0, \\ B^2 = \frac{c_2 d_1 - d_2}{c_1 c_2 - 1}, \quad c_2 d_1 - d_2 > 0. \quad (3.12d)$$

It is a straightforward matter to determine the linear stability of the various solutions and the detail is omitted.

The results of the above analysis are summarized in Figures 10(a)-(d). In Figure 10(a) a perspective view of the situation when $h < H$ is shown. We see that the $(m,1)$ mode, given by (3.12b), bifurcates from the trivial solution at $Ra = Ra_1^*$; this primary branch is stable. At $Ra = Ra_2^*$ there is a further bifurcation to the $(m+1,1)$ mode given by (3.12c) and this mode undergoes secondary bifurcation at $Ra = Ra_3^*$, where

$$Ra_3^* = Ra_H \left\{ 1 - \frac{2(m+1)(h-H)}{(2m+1)^2 H} \right\}.$$

The $(m+1,1)$ mode is unstable for $Ra < Ra_3^*$ but is stabilized by the secondary bifurcation. As $h \rightarrow H$, $(Ra_1^*, Ra_2^*) \rightarrow Ra_H$ and the primary branches approach each other, with the range of Rayleigh number for which the second primary

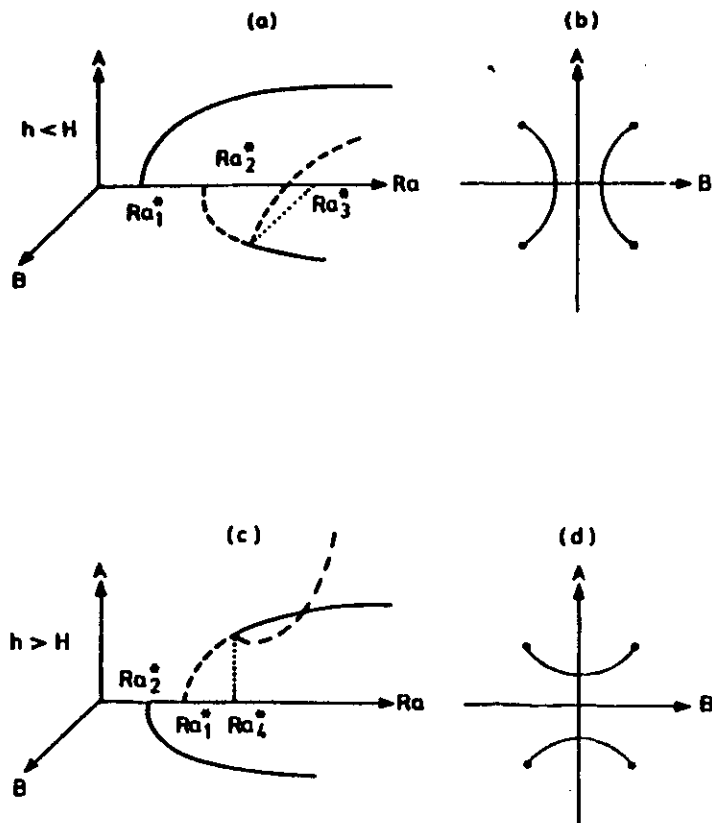


Fig. 10

mode is unstable diminishing. At $h = H$, all the bifurcation points coincide with the pure modes stable and the mixed modes unstable. As h increases further the branches separate again with the $(m+1,1)$ mode becoming the leading primary and with the mixed modes now bifurcating off the $(m,1)$ mode. This situation is shown in Figure 10(c): the $(m+1,1)$ mode bifurcates at $Ra = Ra_2^*$, the $(m,1)$ mode at $Ra = Ra_1^*$. The secondary bifurcation now occurs at $Ra = Ra_4^*$, where

$$Ra_4^* = Ra_{11} \left\{ 1 + \frac{2(6m+5)(h-H)}{(2m+1)^2 H} \right\},$$

leaving the primary mode stable as before.

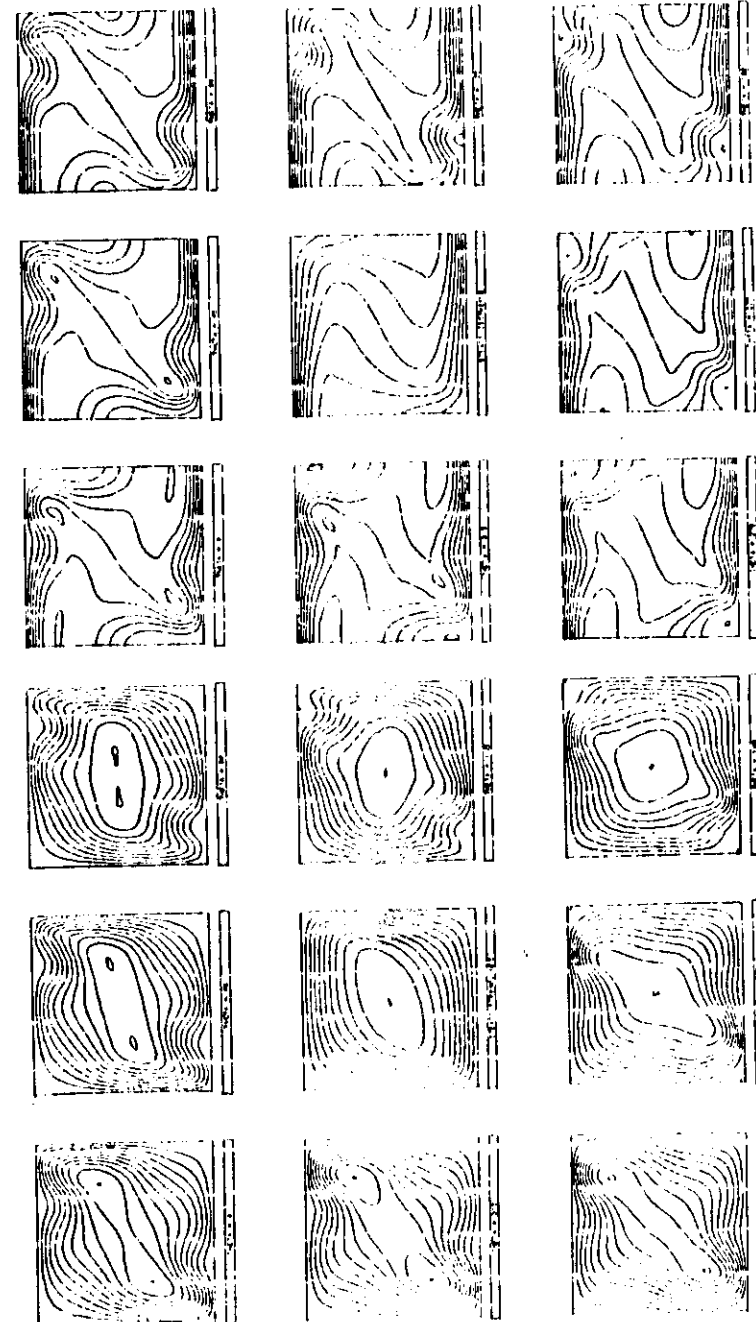
In Figures 10(b), (d) the 'end-on' view along the length of the Rayleigh number axis is displayed in order to clarify the shape of the secondary bifurcation branches. Note that the secondary branches actually continue out infinity but we have truncated them in the figure.

The most important aspect of this analysis is that it reveals that at certain Rayleigh numbers there is more than one stable steady flow. In general engineering systems this feature is crucial, for it shows us that alternative modes of convection, transferring (perhaps) significantly different amounts of heat, exist and must be accounted for in performance assessment and system design studies.

4. Hopf Bifurcation and Route to Chaos

As might be expected, the solutions described above do not remain stable for all high Rayleigh numbers. For example, Kimura, Schubert and Straus [14] have shown that, in a square container, the steady uncellular flow is destabilized by a Hopf bifurcation to a periodic flow,

which is illustrated in figure 11. The instability is caused by a convective instability in the boundary layers that form as ^{the} Rayleigh number increases. In fact, Kimura et al have performed detailed numerical calculations and have mapped out the route to chaos as the Rayleigh number increases. This is a subject of great current research activity, but it lies beyond our immediate concern.



References

1. J. B. Keller, "Darcy's Law for Flow in Porous Media and the Two-Space Method", Nonlinear P.D.E's in Engineering Applied Science, Dekker lecture notes in pure and appl. math., Marcel Dekker Inc., Vol. 54, August 1980.
2. J. Bear and Y. Bachmat, "Advective and Diffusive Fluxes in Porous Media", Proceedings of NATO ASI on Fundamentals of Transport Phenomena in Porous Media.
3. A. E. Scheidegger, "The Physics of Flow Through Porous Media", 3rd Edition, University of Toronto Press, Toronto.
4. J. Bear, "Dynamics of Fluids in Porous Media", Elsevier, New York (1972).
5. P. Forchheimer, "Wasserbewegung Durch Boden", Z. Ver Dt. Ingr., 45, 1782-88 (1901).
6. H. C. Brinkman, "A Calculation of the Viscous Force Exerted by a Flowing Fluid on a Dense Swarm of Particles", Applied Science Research A1, 27-34 (1947).
7. D. A. Nield, "The Boundary Correction to the Rayleigh-Darcy Problem: Limitations of the Brinkman Equation", J. Fluid Mechanics, 128, 37-46 (1983).
8. G. I. Taylor, "Dispersion of Soluble Matter in Solvent Flowing Slowly Through a Tube", Proc. Roy. Soc., A219 186-203, 1953.
9. E. R. Lapwood, "Convection of a Fluid in a Porous Medium", Proc. Camb. Phil. Soc. 44, 508-21 (1948).
10. E. Palm, J. E. Weber and O. Kvernvoid, "On Steady Convection in a Porous Medium", J. Fluid Mech., 54, 153-61 (1972).
11. D. G. Schaeffer, "Qualitative Analysis of a Model for Boundary Effects in the Taylor Problem", Proc. Camb. Phil. Soc., 87, 307 (1980).
12. L. Bauer, H. B. Keller and E. L. Reiss, "Multiple Eigenvalues Lead to Secondary Bifurcation", SIAM Review, 17, 101 (1975).
13. H. Kidachi, "Side Wall Effect on the Pattern Formation of the Rayleigh-Benard Convection", Prog. Theor. Physics, 68, 49 (1982).
14. S. Kimura, G. Schubert and J. M. Straus, "Route to Chaos in Porous-Medium Thermal Convection", J. Fluid Mech. 166, 305-24 (1986).

Other:

S. Bories, "Natural Convection in Porous Media" - Same Source as [2]: good survey article.

R. A. Greenkorn, "Flow Phenomena in Porous Media", Marcel Dekker, Inc. New York (1983).

Acknowledgement

I wish to thank Professor Stephen Davis, for his hospitality at Northwestern University during the preparation of these lectures, and especially, Crystal Whittaker, who interpreted my hieroglyphics and produced such an excellent typed copy.